



**Manchester  
Metropolitan  
University**

---

Wang, L, Zhang, X ORCID logoORCID: <https://orcid.org/0000-0002-8790-0313>, Villarroel, R, Liu, Q, Wang, Z and Zhou, L (2020) Top-oil temperature modelling by calibrating oil time constant for an oil natural air natural distribution transformer. IET Generation, Transmission and Distribution, 14 (20). pp. 4452-4458. ISSN 1751-8687

---

**Downloaded from:** <https://e-space.mmu.ac.uk/626748/>

**Version:** Accepted Version

**Publisher:** Institution of Engineering and Technology (IET)

**DOI:** <https://doi.org/10.1049/iet-gtd.2020.0155>

Please cite the published version

<https://e-space.mmu.ac.uk>

# Top Oil Temperature Modelling by Calibrating Oil Time Constant for an ONAN Distribution Transformer

Lujia Wang<sup>1,2</sup>, Xiang Zhang<sup>1</sup>, Rafael Villarroel<sup>1</sup>, Qiang Liu<sup>1\*</sup>, Zhongdong Wang<sup>1</sup>, Lijun Zhou<sup>2</sup>

<sup>1</sup> Department of Electrical and Electronic Engineering, the University of Manchester, Manchester, UK

<sup>2</sup> School of Electrical Engineering, Southwest Jiaotong University, Chengdu, Sichuan Province, China

\*qiang.liu@manchester.ac.uk

**Abstract:** Integration of low carbon technologies poses a technical challenge on distribution transformers due to the dynamic loading and potentially frequent overloading scenarios. Transformer dynamic thermal rating is hence required, which is the most economical approach to tackle this challenge and ensure the safe operation. To reach the aim, it is important to enhance the accuracy of the dynamic thermal model, where the top oil temperature is a key thermal parameter. In this paper, a wide range of constant load temperature rise tests were carried out on an 11/0.433 kV distribution transformer to study the dynamic thermal behaviour of the top-oil temperature. A model based on the IEC 60076-7 thermal model but with an improved oil time constant calibration was deduced for top oil temperature modelling. The oil time constant calibration was inspired by IEEE C57.91 and verified by 8 temperature rise tests with load factors ranging from 0.7 pu to 1.4 pu. In addition, the improved top-oil temperature modelling was further verified in experiments under multiple load profiles.

## Nomenclature

$C_{th, oil}$	Oil thermal capacity (J/kg).
$I$	Load current (A).
$P$	Loss (W).
$k$	Time step index for discrete calculation.
$R$	Ratio of load loss at rated current to no-load loss.
$\Delta t$	Sampling period (min).
$n$	Oil exponent.
$u$	Constant in Susa's model.

### Greek:

$\theta_{amb}$	Ambient temperature (°C).
$\theta_{oil}$	Top-oil temperature (°C).
$\tau_{oil}$	Top-oil time constant (min).
$\tau_{oil, rated}$	Rated top-oil time constant (min).
$\tau_{aveoil, rated}$	Rated average-oil time constant (min).
$\tau_{oil, pu}$	Relative top-oil time constant.
$\mu$	Oil dynamic viscosity (kg/m·s).
$\Delta\theta_{oil}$	Top-oil rise over ambient temperature (K).
$\Delta\theta_{oil, initial}$	Initial top-oil rise over ambient temperature (K).
$\Delta\theta_{oil, rated}$	Rated top-oil rise over ambient temperature (K).
$\Delta\theta_{oil, ultimate}$	Ultimate top-oil rise over ambient temperature at the load considered (K).

### Abbreviation Subscripts:

$amb$	Ambient.
$pu$	Per unit value.

## 1. Introduction

With increasing implementation of low carbon technologies such as photovoltaic panels (PVs), wind farms and electric vehicles (EVs), etc., overloading of distribution transformers in a local area or within a short period is inevitable due to the volatile nature of the low carbon technologies [1]. Transformer dynamic thermal rating (DTR) is an effective way to tackle the challenge from the

perspective of power system operation and planning. Transformer DTR can fulfil the potential of the transformer by allowing dynamic overloads with real-time estimation of the thermal capacity of the transformer [2], thus being more economical than installing new transformers. For transformer DTR, both hot-spot temperature (HST) and top-oil temperature (TOT) are two important state variables [3, 4].

The vast number of distribution transformers makes it uneconomical to pre-install or re-equip fibre-optic temperature sensors for them. In order to acquire HST and TOT, it is generally the practice to use the loading guides [3, 4] or some other dynamic thermal models [5, 6]. In most dynamic thermal models, HST is calculated as the sum of TOT and hot-spot rise over TOT. As for the hot-spot rise over TOT, the dominant thermal parameters are the hot-spot factor  $H$  [7, 8], average winding to average oil temperature gradient  $gr$  [9], winding time constant  $\tau_w$  [10] and the winding exponent  $m$  [11, 12]. As for the top-oil thermal model, recent reports mainly focus on two aspects: further utilisation of TOT information, and further improvement of TOT calculation accuracy. For the first aim, malfunction of the cooling system or unusual overheating inside the transformer can be detected based on the calculation of TOT standardized error [13, 14]. For the second aim, within the existing modelling framework, the key is to find a group of accurate thermal parameters. If it is for a specific transformer, some algorithms (such as Extended Kalman Filter and Levenberg Marquardt) can fit more than one parameters very well by trained data sets [2], [15]. These parameters, however, turn out to be transformer specific. A universal relationship among the thermal parameters is more useful in the thermal modelling.

In the classic top-oil thermal models (IEC 60076-7 and IEEE C57.91), there are four thermal parameters: the rated top-oil temperature rise, ratio of load loss at rated current to no-load loss, oil exponent and oil time constant. The above parameters directly affect the accuracy of the thermal model output and all of them are transformer specific.

In addition, the oil time constant is dependent on the load and oil temperature. The authors studied the variation of the top-oil time constant under different loads in cold start scenarios [16]. However, in reality, cold-start scenario does not reflect dynamic load conditions. Therefore, considering oil viscosity change with temperature, it is reasonable to assume top-oil time constant to be the initial oil temperature rise related as well.

In this paper, a series of constant load temperature-rise tests were carried out on an 11/0.433 kV distribution transformer. The oil pocket at the top of the tank was selected as the reference location of the top-oil to be in line with practice. The oil exponent was achieved by fitting the steady state temperature-rise test results from 0.7 pu to 1.4 pu. A bidirectional correction method for the top-oil time constant was derived considering both the initial top-oil temperature rise and the load factor, which was directly validated by 8 constant load temperature-rise tests. Based on the initial temperature rise and load factor dependent top oil time constant, the IEC top-oil thermal model was improved and its superiority was demonstrated by comparing with existing top oil models under multiple load profiles.

## 2. Background of Top-oil Thermal Models

### 2.1. Review on Top-oil Thermal Models

The governing differential equations of the widely adopted top-oil thermal models are reviewed in this section.

#### 2.1.1. IEEE C57.91 Clause 7 Model [4]:

The top-oil temperature rise over ambient temperature can be computed as an exponential response from the initial top-oil temperature rise as

$$\left( \frac{1 + RI_{pu}^2}{1 + R} \right)^n \cdot \Delta\theta_{oil, rated} = \tau_{oil, rated} \frac{d\Delta\theta_{oil}}{dt} + \Delta\theta_{oil} \quad (1)$$

and the top-oil temperature is calculated as

$$\theta_{oil} = \Delta\theta_{oil} + \theta_{amb} \quad (2)$$

#### 2.1.2. IEC 60076-7 Model [3]:

On the basis of IEEE model, with the consideration for the effect of ambient temperature variations on top-oil temperature reported by Lesieutre et al. [17], the top-oil temperature calculation was modified as (3).

$$\left( \frac{1 + RI_{pu}^2}{1 + R} \right)^n \cdot \Delta\theta_{oil, rated} = \tau_{oil, rated} \frac{d\theta_{oil}}{dt} + (\theta_{oil} - \theta_{amb}) \quad (3)$$

The drawback of this modification is that no analytical solution for the top oil temperature rise over the ambient temperature is available.

#### 2.1.3. IEC 60076-7 Model with Relative Oil Time Constant [10]:

The authors found that the oil time constants are inversely proportional to the load factor. So the relative oil time constant was proposed to describe this kind of variation. Based on the IEC 60076-7 top-oil thermal model, the relative oil time constant was introduced into the model as

$$\left( \frac{1 + RI_{pu}^2}{1 + R} \right)^n \Delta\theta_{oil, rated} = \left( \frac{1 + RI_{pu}^2}{1 + R} \right)^{n-1} \tau_{oil, rated} \frac{d\theta_{oil}}{dt} + (\theta_{oil} - \theta_{amb}) \quad (4)$$

#### 2.1.4. Thermal-Electrical Analogy Method [5]-[6]:

Swift et al. first adopted the electrical-thermal analogy method for transformer thermal modelling based on the heat transfer theory. In Swift's model, nonlinear thermal resistance was introduced. The differential equation for top-oil temperature can be expressed as (5)

$$\left( \frac{1 + RI_{pu}^2}{1 + R} \right)^{\frac{1}{n}} \cdot \Delta\theta_{oil, rated} = \tau_{oil, rated} \frac{d\theta_{oil}}{dt} + (\theta_{oil} - \theta_{amb})^{\frac{1}{n}} \quad (5)$$

However, Jauregui-Rivera and Amoda et al. conducted an acceptability analysis for the model of Swift and found that Swift's model is not acceptable because it is structurally inaccurate [18,19]. Susa also adopted the electrical-thermal analogy method, which further considers the variation of oil viscosity with temperature [6]. In Susa's approach, top-oil temperature is calculated as

$$\frac{1 + RI_{pu}^2}{1 + R} \cdot \Delta\theta_{oil, rated} = \tau_{oil, rated} \frac{d\theta_{oil}}{dt} + \frac{(\theta_{oil} - \theta_{amb})^{1+u}}{(\mu_{pu} \Delta\theta_{oil, rated})^u} \quad (6)$$

where

$$\mu_{pu} = \exp \left[ \left( \frac{2797.3}{\theta_{oil} + 273} \right) - \left( \frac{2797.3}{\theta_{oil, rated} + 273} \right) \right] \quad (7)$$

### 2.2. Review on Oil Time Constant

In the existing frameworks proposed by IEC and IEEE for the top oil thermal model, there are two key parameters, i.e., the ultimate top oil temperature rise and the oil time constant. Oil exponent proves to be a suitable and robust way to describe the variation of the ultimate oil temperature rise with different loads, leaving the top oil time constant a notion for further improvement. This subsection provides a brief review of oil time constant in the existing thermal models, which are widely adopted in transformer DTR. With respect to different locations inside the tank, the oil time constant could refer to top/average/bottom oil time constant. For distribution transformers, the oil pocket is the most representative and commonly used location to measure the top oil temperature so the top-oil (in the oil pocket) time constant is usually selected as the oil time constant.

#### 2.2.1. Rated Oil Time Constant Estimation:

Oil time constant reflects the changing rate of the oil temperature. For transformers in oil natural air natural (ONAN) cooling modes, the oil time constant is around 200 minutes while it is strongly related to the geometry, thermal design and electrical power loss of the transformer.

For now, the best way to obtain the oil time constant (usually the rated value) is via a non-truncated temperature-rise test [20], where the dynamic oil temperature can be monitored continuously. Some estimation methods were also proposed mainly according to the oil mass and the total loss [3, 4, 6]. In addition, while other modelling methods like thermal-hydraulic network model (THNM) and CFD-based

simulations are effective for steady states [21, 22], these methods are rarely applied in the analysis for the transformer dynamic thermal process.

There are some estimation methods for rated oil time constant. In the IEEE C57.91 Clause 7 model [4] or Susa's model [6], the top-oil time constant can be computed as

$$\tau_{oil,rated} = C_{th,oil} \cdot \frac{\Delta\theta_{oil,rated}}{P_{rated}} \quad (8)$$

where  $C_{th,oil}$  is the oil thermal capacitance and calculated in terms of the cooling type as given in [3, 4, 6].

### 2.2.2. Conversion between Top and Average Oil Time Constants:

According to the report in [23], the top-oil time constant deduced from the rising part of the temperature curve was about half of the simultaneously deduced average-oil time constant. So a correction factor  $k_{11}$  was used to convert between top-oil time constant and average-oil time constant as in [3, 23]

$$\tau_{oil,rated} = k_{11} \cdot \tau_{aveoil,rated} \quad (9)$$

In practice, the top-oil time constant is more commonly used in oil thermal models because top oil temperature is usually readily available, while the average oil time constant requires the often-unknown bottom oil temperature.

### 2.2.3. Correction to Top Oil Time Constant:

The authors proposed the concept of relative thermal time constant (including top-oil time constant and winding time constant) to describe the variation of thermal time constant with load factor for cold start scenarios, where the relative oil time constant was defined as

$$\tau_{oil,pu} = \frac{\tau_{oil}}{\tau_{oil,rated}} \quad (10)$$

Reference [10] provided the deduction process for the relative oil time constant and the expression of the relative oil time constant for cold start scenarios is

$$\tau_{oil,pu} = \left( \frac{1 + RI_{pu}^2}{1 + R} \right)^{n-1} \quad (11)$$

The consideration of relative oil time constant (11) is especially needed in overloading scenarios to avoid significant deviation between predictions and measurements.

Considering variation of the top-oil time constant for any load and for any specific ultimate top-oil rise and the initial top-oil rise, an expression of the relationship between the actual and the rated top-oil time constant is given in IEEE C57.91 as

$$\tau_{oil} = \tau_{oil,rated} \frac{\left( \frac{\Delta\theta_{oil,ultimate}}{\Delta\theta_{oil,rated}} \right) - \left( \frac{\Delta\theta_{oil,initial}}{\Delta\theta_{oil,rated}} \right)}{\left( \frac{\Delta\theta_{oil,ultimate}}{\Delta\theta_{oil,rated}} \right)^{\frac{1}{n}} - \left( \frac{\Delta\theta_{oil,initial}}{\Delta\theta_{oil,rated}} \right)^{\frac{1}{n}}} \quad (12)$$

where the constant  $n$  takes different values based on cooling modes as given in [4]. If  $n$  is less than 1, the time constant must be modified with (12) for overloaded cycles.

## 3. Experimental Set-up and Results

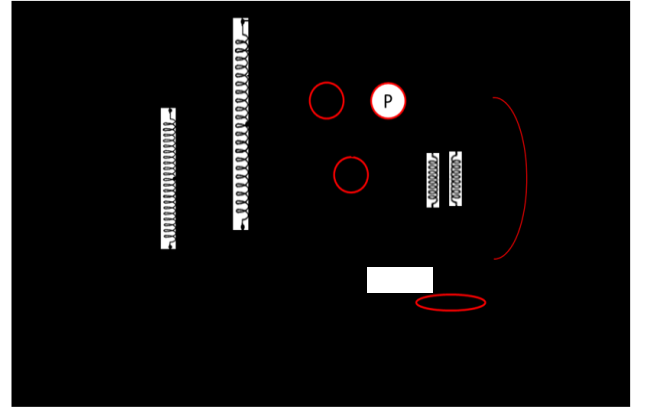
The top-oil time constant is derived from the dynamic process under a fixed load and oil exponents are from steady-state temperature-rise-test results. Therefore, conducting temperature-rise tests with a wide range of load factors is the best way to investigate the above two thermal parameters.

### 3.1. Tested Transformer and Experimental Setup

The transformer used in this work is a 200 kVA, 11/0.433 kV distribution transformer with an oil-natural air-natural (ONAN) cooling mode and is filled with mineral oil [24]. The transformer is a three-phase 3-limb core-type transformer with layer-type windings connected in Dyn11. The rated load loss and no-load loss from factory tests are 2500W and 257W, respectively. During the temperature rise tests, four thermocouples were placed around the transformer to monitor the ambient temperature.

A series of temperature-rise tests of the transformer was carried out according to IEC 60076-2 [25], where the short-circuit method was used as indicated in Fig. 1 (a). A photo of the test setup including the transformer to be tested, the variac, the step-up transformer and other auxiliary equipment is shown in Fig. 1 (b). During the test, the low-voltage terminals of the transformer were short circuited using a solid copper link, and the transformer is then subjected to a test current corresponding to the calculated total losses (load losses plus no-load losses).

These tests can be divided into two groups: constant-load temperature-rise tests and dynamic-load temperature-rise tests. Constant-load temperature-rise tests were used to acquire the input parameters for the thermal model such as the rated oil temperature, the oil exponent and the oil time constants and dynamic temperature-rise tests were applied to verify the improved thermal model as well as the validity of the derived thermal parameters.



(a)



(b)

**Fig. 1.** Experimental setup of temperature-rise tests: (a) schematic testing circuit diagram; (b) a photo of the test setup.

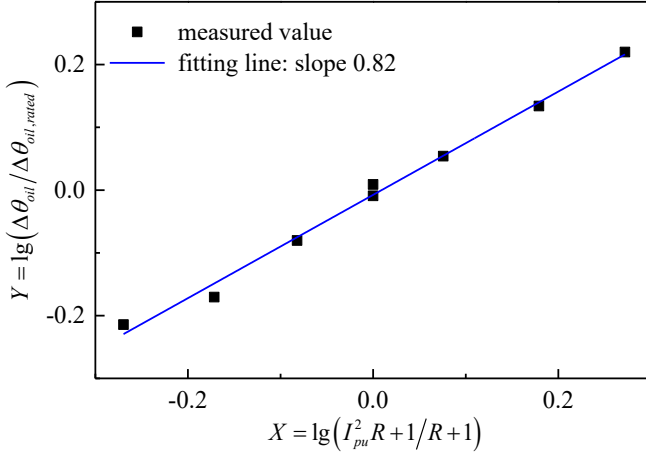


**Fig. 2.** Regression estimation for oil exponent of oil pocket temperature under different load levels.

### 3.2. Steady State Oil Temperature Rise and Oil Exponent

According to IEC 60076-2, the top-oil temperature rise is established when the transformer is subjected to a test current corresponding to the total losses of transformer. The first part of the test can be terminated when the rate of change of top-oil temperature rise has fallen below 1 K per hour and has remained there for a period over three hours. For distribution transformers, the top-oil temperature is conventionally determined by one sensor immersed in the insulating liquid at the top of the tank or, in the oil pocket in the cover. In our tests, from 0.7 pu to 1.4 pu, the top-oil temperature rises over ambient temperature in the oil pocket are presented in Table 1.

As recommended by IEC 60076-7 and IEEE C57.91, the definition for the oil exponent  $n$  is presented as (13)

$$\Delta\theta_{oil} = \Delta\theta_{oil,rated} \left( \frac{I_{pu}^2 R + 1}{R + 1} \right)^n \quad (13)$$

In (13), there is a strong non-linear relationship between the top-oil temperature rise over ambient temperature and the total loss. In order to use linear regression to fit the oil exponent, we take the common logarithm on both sides of (13) [26]

$$\lg\left(\frac{\Delta\theta_{oil}}{\Delta\theta_{oil,rated}}\right) = n \lg\left(\frac{I_{pu}^2 R + 1}{R + 1}\right) \quad (14)$$

let the variable  $Y = \lg(\Delta\theta_{oil} / \Delta\theta_{oil,rated})$ , and let the variable  $X = \lg(I_{pu}^2 R + 1 / (R + 1))$ . Based on (14) with information shown in Table 1, the fitting curve for oil exponent was plotted for a load range from 0.7 pu to 1.4 pu, as shown in Fig. 2. The slope of the fitting curve is 0.82, which approximately equals the recommended value of 0.8 in [3]-[4].

### 3.3. Dynamic Oil Temperature Rise and Oil Time Constant

The relative relationship between the oil time constants in different load conditions is useful to dynamic thermal modelling. The authors already reported that the top-oil time constant varies with load factor in cold start

**Table 1** Oil temperature rises at oil pocket under different load currents

No.	Load current per unit	Oil temperature rise at oil pocket / K
1	0.7	23.5
2	0.8	26.0
3	0.9	32.0
4	1.0	37.7
5	1.0	39.3
6	1.1	43.6
7	1.25	52.4
8	1.4	63.9

conditions and proposed the relative thermal time constants (RTTC) to describe this variation [10]. It is also expected that the initial top oil temperature rise can affect the time constant according to (12) [4].

Eight non-truncated temperature-rise tests were conducted to obtain the top-oil temperature curves as shown in Fig. 3. A non-truncated temperature-rise test means that the transformer is subjected to a test current corresponding to a constant load current until reaching the steady state [20], [27]. In the process, the top-oil temperature was recorded continuously. In order to extrapolate the oil time constant, the fitting format, as shown in (15) was used to fit these curves.

$$\Delta\theta_{oil}(t) = (\Delta\theta_{oil,ultimate} - \Delta\theta_{oil,initial}) \times \left( 1 - e^{-\frac{t}{\tau_{oil}}} \right) + \Delta\theta_{oil,initial} \quad (15)$$

The load current per unit, the initial oil temperature rises and corresponding fitting results from Fig. 3 are presented in Table 2.

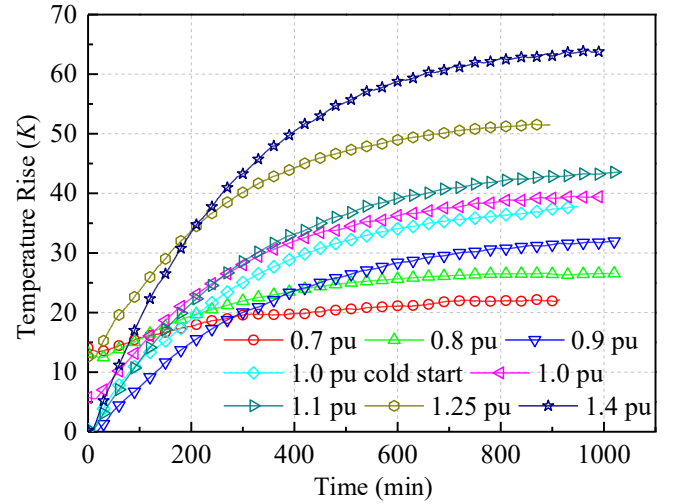


**Fig. 3.** Oil temperature rise curves monitored from non-truncated heat run tests under different constant loads with initial temperature rises.

**Table 2** Oil time constants fitted from temperature-rise tests and normalized oil time constants

No	$I_{pu}$	$\Delta\theta_{oil, initial} / K$	Fitting from measured top-oil (in oil pocket) temperature		Normalized oil time constant		
			$\tau_{oil} / \text{min}$	Adj. R-Square	Measured $\tau_{oil, pu}$	$\tau_{oil, pu}$ by (16)	$\tau_{oil, pu}$ by (17)
1	0.7	14.1	290.9	0.9903	0.989	1.118	0.957
2	0.8	13.1	267.4	0.9952	0.909	1.074	0.937
3	0.9	0.0	313.8	0.9997	1.066	1.035	1.038
4	1.0	0.3	<b>294.3</b>	0.9994	<b>1.000</b>	1.000	0.994
5	1.0	5.7	281.1	0.9993	0.955	1.000	0.937
6	1.1	0.5	292.6	0.9942	0.994	0.969	0.962
7	1.25	12.6	253.3	0.9995	0.861	0.929	0.841
8	1.4	0.2	270.9	0.9204	0.920	0.893	0.891

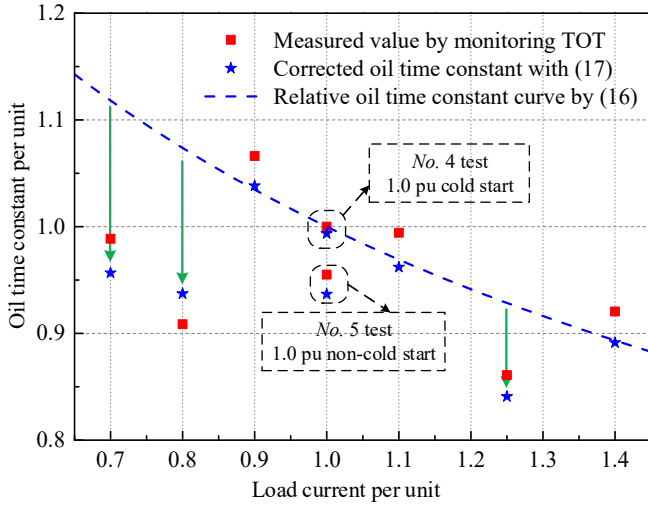


**Fig. 4.** Normalized oil time constants comparisons among measured values, relative oil time constants by (16) and corrected oil time constants by (17) from 8 non-truncated heat run tests.

#### 4. Correction for Oil Time Constant

##### 4.1. Effect of Initial Oil Temperature on Oil Time Constant

Two tests under rated load were conducted. One was with negligible initial top oil temperature rise (No. 4 in Table 2) and the other with an initial top oil temperature rise of 5.7 K (No. 5 in Table 2) due to not enough time for the top oil to cool down to ambient temperature from its previous temperature-rise test. The initial temperature rise results in a reduced top oil time constant as shown in Table 2. This is because higher temperature leads to lower viscosity and therefore shorter time required to reach a steady state.

##### 4.2. Correction for Oil Time Constant Considering the Effect of Initial Oil Temperature Rise

If only consider the load dependent nature of oil time constants, the relative top-oil time constant can be expressed as [10]

$$\tau_{oil, pu}(I_{pu}) = \left( \frac{1 + RI_{pu}^2}{1 + R} \right)^n \left/ \left( \frac{1 + RI_{pu}^2}{1 + R} \right) \right. \quad (16)$$

As inspired by (12) in IEEE C57.91 Clause 7 to consider the initial oil temperature, (16) is expanded to (17)

$$\tau_{oil, pu}(I_{pu}, \Delta\theta_{oil, initial}) = \frac{\left( \frac{1 + RI_{pu}^2}{1 + R} \right)^n - \left( \frac{\Delta\theta_{oil, initial}}{\Delta\theta_{oil, rated}} \right)}{\left( \frac{1 + RI_{pu}^2}{1 + R} \right) - \left( \frac{\Delta\theta_{oil, initial}}{\Delta\theta_{oil, rated}} \right)^{\frac{1}{n}}} \quad (17)$$

In order to verify (17), the fitted top-oil time constants in Table 2 are normalized against 294.3 min (No. 4 test), which is the rated top-oil time constant with a cold start. The normalized top-oil time constants, the calculated relative top-oil time constants considering the initial oil temperature rise by (17), and the relative top-oil time constant curve plotted based on (16) are compared in Fig. 4 and listed in Table 2. According to (17), the relative oil time constant variation with load factor in different ratio of  $\Delta\theta_{oil, initial} / \Delta\theta_{oil, rated}$  was plotted in Fig. 5.

From Fig. 4, it is clear that the top-oil time constants calculated by (17) are much closer to experimental results. The green line segments with an arrow show the extent of accuracy that can be achieved by considering initial top oil temperature rise compared to the estimation from (16). Fig. 5 shows a consistent decreasing trend of the oil time constant with either a higher initial oil temperature rise or a higher ultimate temperature rise due to a higher load factor.

Besides the direct comparisons of time constant shown in Fig. 4, the influence of different time constant modifications on top oil temperature prediction are presented in the following section.

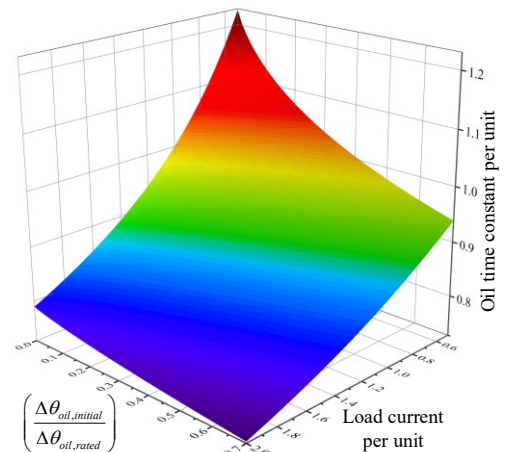


**Fig. 5.** Oil time constant per unit (relative oil time constant) variation with load current per unit in different ratio of initial oil temperature rise to rated oil temperature rise.

## 5. Improved IEC Thermal Model and Verification

### 5.1. Improved IEC Top-oil Thermal Model

IEC 60076-7: 2005 and IEC 60076-7: 2018 both calculate the top-oil temperature using a first-order differential equation, which is a partly improved model to IEEE C57.91 Clause 7 model to account for ambient temperature variation.

The improved differential equation can be obtained with the oil time constant calibration (17) based on (3) as

$$\frac{\left(\frac{1+RI_{pu}^2}{1+R}\right)^n - \left(\frac{\theta_{oil} - \theta_{amb}}{\Delta\theta_{oil,rated}}\right)}{\left(\frac{1+RI_{pu}^2}{1+R}\right) - \left(\frac{\theta_{oil} - \theta_{amb}}{\Delta\theta_{oil,rated}}\right)^n} \tau_{oil,rated} \frac{d\theta_{oil}}{dt} = \left(\frac{1+RI_{pu}^2}{1+R}\right)^n \Delta\theta_{oil,rated} + (\theta_{oil} - \theta_{amb}) \quad (18)$$

where the term  $\Delta\theta_{oil, initial}$  has been replaced with the term  $\theta_{oil} - \Delta\theta_{amb}$ . Since (18) was introduced for discretised calculation based on sampling period, a discrete-time form of (18) with Euler approximation can be derived as

$$\theta_{oil}(k) = \frac{\tau_{oil}}{\tau_{oil} + \Delta t} \theta_{oil}(k-1) + \frac{\Delta t}{\tau_{oil} + \Delta t} \theta_{amb}(k) + \frac{\Delta t}{\tau_{oil} + \Delta t} \left[ \frac{1+RI_{pu}^2(k)}{1+R} \right]^n \Delta\theta_{oil,rated} \quad (19)$$

where the varying oil time constant  $\tau_{oil}$  should be substituted with the product of  $\tau_{oil,rated}$  and  $\tau_{oil,pu}$  according to (10). As for the relative oil time constant  $\tau_{oil,pu}$  (17), it should be noted that the initial oil temperature rise in (17) is  $\theta_{oil}(k-1) - \theta_{amb}(k-1)$  from last iteration while the load current per unit in (17) is  $I_{pu}(k)$ , namely as

$$\tau_{oil,pu} = \frac{\left[\frac{1+RI_{pu}^2(k)}{1+R}\right]^n - \left[\frac{\theta_{oil}(k-1) - \theta_{amb}(k-1)}{\Delta\theta_{oil,rated}}\right]}{\left[\frac{1+RI_{pu}^2(k)}{1+R}\right] - \left[\frac{\theta_{oil}(k-1) - \theta_{amb}(k-1)}{\Delta\theta_{oil,rated}}\right]^n} \quad (20)$$

### 5.2. Verifications

#### 5.2.1 Case 1 Changing Load Temperature-rise Test:

The changing load profile, ambient temperature, measured TOT, calculated TOTs from different differential models implemented in MATLAB and evolution of oil time constants are presented in Fig. 6.

As in Table 3, Group a is based on the improved model (18); Group b is based on the model (4) in [10]; Group c is based on the original IEC model (3). They all use the same oil exponent of 0.82.

Error curves are also presented in Fig. 6. All errors are those measured values minus calculated values. To further quantify the errors between the measured TOT and the calculated TOT from different models, the root mean square error (RMSE) is used as

$$RMSE = \sqrt{\frac{1}{N} \sum_{i=1}^N [\theta_{oil,measured}(t_i) - \theta_{oil,calculated}(t_i)]^2} \quad (21)$$

where  $N$  is the number of readings;  $\theta_{oil, measured}(t_i)$  and  $\theta_{oil, calculated}(t_i)$  are the measured TOT and the calculated TOT, respectively. For group a to c, their RMSEs are 0.47, 0.69 and 0.72, respectively, as shown in Table 3, which indicates group a is the best estimation among the three groups. Since the average load level is low, the temperature rise is small, and all RMSEs are quite small. The superiority of equation (18) is achieved by taking into account both initial and ultimate temperature rise in each load step.

#### 5.2.2 Case 2: Step-change Overloading Temperature-rise Test:

The step-change overloading profile (0.7-1.8-0.7), temperatures, and error curves and evolution of oil time constants are presented in Fig. 7 for the same three groups with the same oil exponent of 0.82. For group a to c, their RMSEs are 0.72, 0.88 and 1.84 as shown in Table 3, which also indicates group a results in the best estimation among the 3 groups.

For the step-change overloading condition, a constant time constant as in the IEC model, equation (3), results in significant underestimation of the top oil temperature. The modification of the time constant based only on the ultimate temperature rise, i.e. the load factor, as in equation (16), leads to abrupt changes of the time constant and corresponding overshooting results. On the other hand, the time constant modification with the consideration of both initial and ultimate temperature rises, equation (18), smooths the time constant evolution and results in a quick comeback to the measured value after the load excursion. For the overloading condition, the modification of the time constant based only on load factor is still effective since at this condition the load factor is dominating. Overall, the top oil dynamic thermal model shown by (18) is the best due to its comprehensive oil time constant calibration for both initial and ultimate oil temperature rises.

**Table 3** Input thermal parameters for group a, b, c and calculation results comparison using RMSE

$\Delta\theta_{oil,rated}$	38.4 K	$R$	9.73
$n$	0.82	$\tau_{oil,rated}$	294.3 min
$RMSE$	Group a: eq. (18)	Group b: eq. (4)	Group c: eq. (3)
Changing load profile test	0.47	0.69	0.72
Step-change overloading profile test	0.72	0.88	1.84



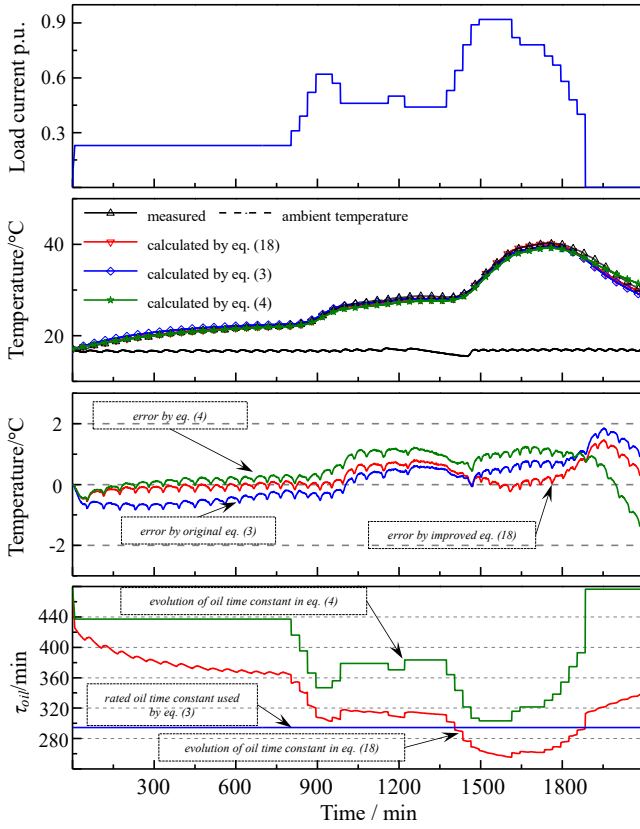


**Fig. 6.** Verification results under changing load profile: (a) loading profile; (b) top-oil temperatures during the changing load temperature-rise test; (c) errors produced by different top-oil thermal model; (d) comparisons for the evolution of oil time constant among different top-oil thermal model.

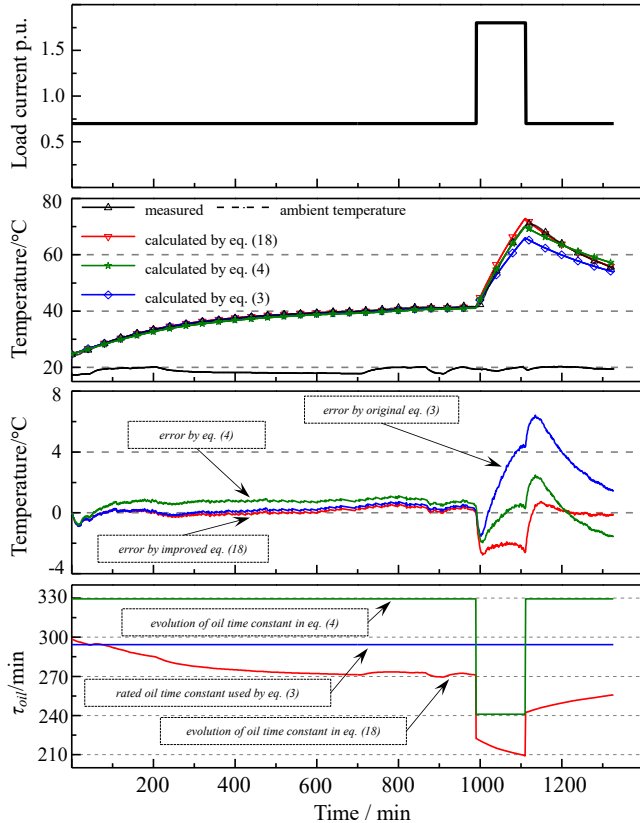


**Fig. 7.** Verification results under step-change overloading profile: (a) loading profile; (b) top-oil temperatures during the steps load heat run test; (c) errors produced by different top-oil thermal model; (d) comparisons for the evolution of oil time constant among different top-oil thermal model.

## 6. Conclusion

Temperature-rise tests of a distribution transformer with a wide range of load factors were conducted to better understand TOT dynamics. The main conclusions were drawn:

1) The steady state TOTs were found well estimated by the oil exponent method with the exponent being 0.82 as derived from curve fitting of the measured data.

2) An oil time constant calibration method based on IEEE C57.91 was implemented considering both the initial oil temperature rise and the load factor. This was verified by 8 heat run tests with load factor ranging from 0.7 to 1.4.

3) The need to incorporate such an oil time constant calibration into the IEC top-oil thermal model is demonstrated by additional thermal tests under a changing load profile test and a step-change overloading profile.

## 7. Acknowledgments

This work was funded by the Engineering and Physical Sciences Research Council (EPSRC) through the Innovate UK consortium project “Common Application Platform for Low Voltage Network Management”, grant number EP/N508421/1. Lujia Wang, would like to express his gratitude to China Scholarship Council for providing visiting PhD student scholarship under Grant number 201807000033.

## 8. References

- [1] Gao, Y., Patel, B., Liu, Q., Wang, Z., and Bryson, G.: “Methodology to assess distribution transformer thermal capacity for uptake of low carbon technologies,” IET Gener. Transm. Distrib., vol. 11, no. 7, May. 2017, pp. 1645-1651
- [2] Alvarez, D.L., Rivera S.R., and Mombello, E.E.: “Transformer thermal capacity estimation and prediction using dynamic rating monitoring,” IEEE Trans. Power Del., vol. 34, no. 4, Aug. 2019, pp. 1695-1705
- [3] IEC 60076-7: “Power Transformers - Part 7: Loading Guide for Oil-Immersed Power Transformers”, 2005
- [4] IEEE Standard C57.91-1995: “IEEE Guide for Loading Mineral-Oil-Immersed Transformers and Step-Voltage Regulators”, 2011
- [5] Swift, G., Molinski, T.S., and Lehn, W.: “A fundamental approach to transformer thermal modeling-I. Theory and equivalent circuit,” IEEE Trans. Power Del., vol. 16, no. 2, Apr. 2001, pp. 171-175
- [6] Susa, D., and Lehtonen, M.: “Dynamic thermal modelling of power transformers: further development - part I,” IEEE Trans. Power Del., vol. 21, no. 4, Oct. 2006, pp. 1961-1970
- [7] Zhang, X., Wang, Z., and Liu, Q.: “Interpretation of hot spot factor for transformers in OD cooling modes,” IEEE Trans. Power Del., vol. 33, no. 3, Jun. 2018, pp. 1071-1080
- [8] Feng, D., Wang, Z., and Jarman, P.: “Evaluation of power transformers effective hot-spot factors by thermal



- modelling of scrapped units,” *IEEE Trans. Power Del.*, vol. 29, no. 5, Oct. 2014, pp. 2077-2085
- [9] Wang, L., Zhou, L., Yuan, S., Wang, J., Tang, H., and Guo, L.: “Improved dynamic thermal model with pre-physical modelling for transformers in ONAN cooling mode,” *IEEE Trans. Power Del.*, vol. 34, no. 4, Aug. 2019, pp. 1442-1450
- [10] Wang, L., Zhou, L., Tang, H., Wang, D., and Cui, Y.: “Numerical and experimental validation of variation of power transformers’ thermal time constants with load factor,” *Appl. Therm. Eng.*, vol. 126, Nov. 2017, pp. 939-948
- [11] Douglas, D.H., Lawrence C.O., and Templeton, J.B.: “Factory overload testing of a large power transformer,” *IEEE Trans. Power Appar. Syst.*, vol. PAS-104, no. 9, 1985, pp. 2492-2500
- [12] Peterchuck, D., and Pahwa, A.: “Sensitivity of transformer’s hottest-spot and equivalent aging to selected parameters,” *IEEE Trans. Power Del.*, vol. 17, no. 4, Oct. 2002, pp. 996-1001
- [13] Djamali, M., and Tenbohlen, S.: “A validated online algorithm for detection of fan failures in oil-immersed power transformers,” *Int. J. Therm. Sci.*, vol. 116, 2017, pp. 224-233
- [14] Djamali, M., and Tenbohlen, S.: “Malfunction detection of the cooling system in air-forced power transformers using online thermal monitoring,” *IEEE Trans. Power Del.*, vol. 32, 2017, pp. 1058-1067
- [15] Najjar, S., Tissier, J.F., Cauet, S., and Etien, E.: “Improving thermal model for oil temperature estimation in power distribution transformers,” *Appl. Therm. Eng.*, vol. 119, 2017, pp. 73-78
- [16] Wang, L., Zhou, L., Wang, D., Tang, H., and Guo, L.: “Impact of overload pickup on dynamic hot-spot temperature rise in traction transformer,” *Proc. Chinese Soc. Electr. Eng. (CSEE)*, vol. 37, no. 24, Dec. 2017, pp. 7350-7358 (in Chinese)
- [17] Lesieutre, B.C., Hagman, W.H., and Kirtley, J.L.: “An improved transformer top oil temperature model for use in an on-line monitoring and diagnostic system,” *IEEE Trans. Power Del.*, vol. 12, no. 1, Jan. 1997, pp. 249-256
- [18] Jauregui-Rivera L., and Tylavsky, D.J.: “Acceptability of four transformer top-oil thermal models—part I: defining metrics,” *IEEE Trans. Power Del.*, vol. 23, 2008, pp. 860-865
- [19] Amoda, A., Tylavsky, D.J., McCulla, G.A., and Knuth, W.A.: “Acceptability of three transformer hottest-spot temperature models,” *IEEE Trans. Power Del.*, vol. 27, no.1, Jan. 2012, pp. 13-22
- [20] Susa D., and Nordman, H.: “IEC 60076-7 loading guide thermal model constants estimation,” *Int. T. Elect. Energy*, vol. 23, 2013, pp. 946–960
- [21] Zhang, J., and Li, X.: “Oil cooling for disk-type transformer windings-part 1: theory and model development,” *IEEE Trans. Power Del.*, vol. 21, Jul. 2006, pp. 1318-1325
- [22] Zhang, X., Daghray, M., Wang, Z., Liu, Q., Jarman, P., and Negro, M.: “Experimental verification of dimensional analysis results on flow distribution and pressure drop for disc-type windings in OD cooling modes,” *IEEE Trans. Power Del.*, vol. 33, Aug. 2018, pp. 1647-1656
- [23] Nordman, H., Rafsback, N., and Susa, D., “Temperature responses to step changes in the load current of power transformers,” *IEEE Trans. Power Del.*, vol. 18, no. 4, Oct. 2003, pp. 1110–1117
- [24] Villarroel, R., Liu, Q., and Wang, Z.: “Experimental study of dynamic thermal behaviour of an 11 kV distribution transformer,” in *CIREN - Open Access Proceedings Journal*, vol. 2017, no. 1, 2017, pp. 158-162
- [25] IEC 60076-2: “Power Transformers - Part 2: Temperature rise for liquid-immersed transformers”, 2011.
- [26] Zhou, L., Wang, L., Tang, H., Wang, J., Guo, L., and Cui, Y.: “Oil exponent thermal modelling for traction transformer under multiple overloads,” *IET Gener. Transm. Distrib.*, vol. 12, no. 22, 2018, pp. 5982-5989
- [27] IEEE Standard C57.119: “IEEE Recommended Practice for Performing Temperature Rise Tests on Liquid-Immersed Power Transformers at Loads Beyond Nameplate Ratings”, 2018